Tellus (1988), *40A*, 398–406

Unsteady atmospheric vortices in a stratified atmosphere

By C. SOZOU, *Department of Applied & Computational Mathematics, The University, Sheffield S10 2TN, England*

(Manuscript received 22 June 1987; in final form 8 December 1987)

ABSTRACT

Similarity equations relating to unsteady vortices in a stratified atmosphere are re-examined. A spectrum of solutions wider than hitherto reported in the literature has been found. The solutions relate to one- and two-cell vortices such that the radial and axial velocities are zero at large distances from the axis of the vortex. Far from the axis, the radial velocity is directed to the axis, whereas close to the axis, it can be directed towards the axis (for one-cell solutions) or away from it (for two-cell solutions). The axial velocity can be an up-draught or a system of up-draughts and down-draughts. It is also shown that small changes in the azimuthal velocity can result in large changes in the vertical and radial velocities of the system.

1. Introduction

It is generally believed that intense atmospheric vortices, such as tornadoes, are caused by the convergence of background angular momentum which generates an up-draught that results in radial mass flow. Due to the complexity of the problem simplifying assumptions are usually made in order to understand particular features of it. To that end, Kuo (1966) constructed similarity solutions relating to steady axisymmetric vortices in a stratified atmosphere. The solutions constructed exhibit features of tornado vortices and for certain parameters the tangential velocities correlate well with observational results as found, for example, in the article by Davies-Jones (1986). Kuo's work was extended to unsteady regimes by Kendall (1978) who pointed out that these solutions have certain physical weaknesses. The vertical velocity is proportional to the height above the ground. The radial and azimuthal velocities are independent of the vertical coordinate and therefore are not zero on the ground. Also at large distances r from the axis of the system, at a particular time, the radial mass inflow increases and tends to infinity as $r \to \infty$ and the vertical velocity w is constant instead of zero. Bellamy-Knights and Saci (1983) constructed a one-cell analytical solution of the appropriate nonlinear equations that removes the last difficulty, that is they constructed a one-cell analytical solution such that as $r \to \infty$ the radical mass inflow is a constant and w tends to zero. In this model the axial velocity w is directed away from the ground everywhere. A one-cell solution relates to a system where the radial velocity u does not change sign. A solution such that u changes sign once represents a two-cell vortex. These similarity solutions provide mainly qualitative information and can be relevant away from the ground where the frictional ground effects are unimportant. The physical configuration has sufficient flexibility to make one suspect that there is a wider range of solutions that reveal more structural details of the vortex than hitherto reported in the literature. A numerical solution of the equations confirmed our ideas. We found a set of one- and a set of two-cell solutions such that u and w tend to zero as $r \to \infty$. When certain parameters of the problem tend to limiting values the solutions diverge.

2. General equations of the problem

We use a cylindrical polar coordinate system (r, ϕ, z) with the z-axis along the axis of symmetry of the problem. The origin is on the ground and

$z \geqslant 0$ denotes the distance from the ground. The pressure and density of the fluid are denoted by p and ρ and the components of the velocity in the radial, azimuthal and z-directions by u, v and w, respectively. The problem is axisymmetric and the system of equations relating to the basic and unstable configurations was developed by Kuo and will not be repeated here. Some of the lengthy details of the derivation of these equations can also be found in the paper by Bellamy-Knights and Saci who used a slightly different notation from that of Kuo. Very briefly the procedure is as follows.

Let H and h denote the heights of the atmosphere and the unstable layer, respectively. Introduce dimensionless variables R, Z and t' and the parameters α, ξ by

$$R = r/h, \quad Z = z/h, \quad t' = Vt/h,$$
$$\alpha = h/H, \quad \xi = V^2/gh,$$

where V is a reference velocity and g the acceleration due to gravity and the parameters α and ξ satisfy the condition α, $\xi \ll 1$. Then non-dimensionalise the flow and thermodynamic variables, expand them in powers of α and $\xi \ll 1$ and substitute in the momentum and entropy equations. To the first order in ξ and zeroth order in α these equations yield

$$\frac{Du_0}{Dt'} - \frac{M_0^2}{R^3} = -\frac{H_0}{h}\frac{\partial p_1}{\partial R} + \nu_1\left(\nabla_1^2 - \frac{1}{R^2}\right)u_0, \tag{1}$$

$$\frac{DM_0}{Dt'} = \nu_1\left(\nabla_1^2 - \frac{2}{R}\frac{\partial}{\partial R}\right)M_0, \tag{2}$$

$$\frac{Dw_0}{Dt'} = -\frac{H_0}{h}\frac{\partial p_1}{\partial Z} + s_1 + \nu_1 \nabla_1^2 w_0, \tag{3}$$

$$\frac{Ds_1}{Dt'} - a w_0 = k_1 \nabla_1^2 s_1, \tag{4}$$

$$\frac{D}{Dt'} = \frac{\partial}{\partial t'} + u_0\frac{\partial}{\partial R} + w_0\frac{\partial}{\partial Z} \quad \text{and}$$

$$\nabla_1^2 = \frac{\partial^2}{\partial R^2} + \frac{1}{R}\frac{\partial}{\partial R} + \frac{\partial^2}{\partial Z^2},$$

where u_0, v_0 and w_0 are the values of u/V, v/V and w/V, respectively, correct to order ξ^0, $M_0 = Rv_0$, $H_0 = R_d T_\infty/g$, R_d being the gas constant for air and T_∞ the basic state temperature at ground level. The perturbation pressure correct to order ξ is $(p_\infty V^2/gh)p_1$, p_∞ being the basic state pressure at ground level and $s_1\xi$ is the dimensionless perturbation entropy correct to order ξ. The constants ν_1 and k_1 are defined by $\nu_1 = \nu/hV$, $k_1 = k/hV$, where ν and k are the eddy viscosity and eddy conduction coefficients. The parameter a is defined in Kuo's equation (3.1c). Note that our u_0, v_0, w_0, p_1, s_1 and M_0 correspond to the parameters u_{00}, v_{00}, w_{00}, p_{10}, s_{10} and M_{00} in Kuo's paper. Also our u_0, w_0, p_1 and s_1 are identical to the corresponding parameters in the paper by Belamy-Knights and Saci.

The continuity equation can be approximated by

$$\frac{\partial}{\partial R}(Ru_0) + \frac{\partial}{\partial Z}(Rw_0) = 0. \tag{5}$$

Bellamy-Knights and Saci showed that, for a suitable choice of variables, eqs. (1)-(5) have similarity solutions. Here we shall use the slightly more general variables employed by Kendall. We set

$$\eta = \frac{R^2}{c_1 + 4\nu_1 t'}, \quad u_0 = -\frac{2\nu_1}{R}f(\eta),$$

and then (5) yields

$$w_0 = \frac{4\nu_1 Z f'(\eta)}{c_1 + 4\nu_1 t'}.$$

We also set

$$M_0 = M_0(\eta), \quad p_1 = \frac{4\nu_1 \bar{p}_1(\eta)}{c_1 + 4\nu_1 t'},$$
$$s = \frac{16\nu_1^2 Z\sigma(\eta)}{(c_1 + 4\nu_1 t')^2},$$

and assume that

$$a = a_0\left(\frac{c_1 + 4\nu_1 t_0'}{c_1 + 4\nu_1 t'}\right)^2 = \frac{16\nu_1^2 A^2}{(c_1 + 4\nu_1 t')^2},$$

where $A^2 = a_0(t_0' + c_1/4\nu_1)^2$, a_0 being a constant. The parameter $t_0' = Vt_0/h$ is a reference time and the constant c_1 satisfies the condition $c_1 \geqslant 0$. Using these relationships we can transform equations (1)-(4), respectively, to

$$\bar{p}' = \frac{h\nu_1}{H_0}\left[\frac{M_0^2}{8\nu_1^2\eta^2} - f' - f'' - \left(\frac{f^2}{2\eta}\right)'\right], \tag{6}$$

$$\eta M_0'' + fM_0' + \eta M_0' = 0, \tag{7}$$

$$(\eta f'')' + (\eta f')' + ff'' - f'^2 + \sigma = 0, \tag{8}$$

$$\left(\frac{k_1}{\nu_1}\right)(\eta\sigma')' + (\eta\sigma)' - f'\sigma + f\sigma' + A^2 f' + \sigma = 0. \tag{9}$$

Eqs. (6)–(9) were originally derived by Bellamy-Knights and Saci with $c_1 = 0$, $a_0 = 1$. Eqs. (8) and (9) must be solved subject to the boundary conditions

$$f(0) = 0, \quad f'(\infty) = 0, \quad \sigma(\infty) = 0.$$

When $f(\eta)$ is constructed we can substitute in (7) and solve for M_0 subject to

$$M_0(0) = 0, \quad M_0(\infty) = \text{finite constant}$$

and we can then integrate (6) for the pressure field.

The parameter v_1/k_1 is the turbulent Prandtl number which for atmospheric vortices is of order unity. Bellamy-Knights and Saci set $k_1 = v_1$ and assumed that $\sigma = cf'$, where c is a constant. They also imposed the condition

$$c^2 - c - A^2 = 0, \tag{10}$$

in which case (8) and (9) reduce to the same equation, namely

$$(\eta f'' + \eta f')' + ff'' - f'^2 + cf' = 0. \tag{11}$$

3. Solutions and discussion

Bellamy-Knights and Saci constructed the following closed form solution of (11)

$$f = c(1 - e^{-\eta}), \tag{i}$$

which satisfies all the boundary conditions. This is evidently a one-cell solution and relates to an axial velocity which is positive everywhere. These authors also mention the analytic solutions

$$f = (1 + c)\eta, \tag{ii}$$

$$f = (1 + c)\eta - \frac{2c + 3}{c + 2}[1 - e^{-(c+2)\eta}], \tag{iii}$$

which do not satisfy the boundary condition $f'(\infty) = 0$. The solution (iii) was constructed by Kendall (his equation (30)). Here Kendall's $b = (c + 1.5)/(c + 2)$ and his $c(t)x = (c + 2)\eta$.

The solution (i) was discussed in detail by Bellamy-Knights and Saci (1983). It seemed to us that one might be able to construct numerically more general solutions to (11) than (i) which satisfy all the boundary conditions of the problem.

Eq. (11) can be solved by forward integration. To start off the solution we must specify f, f' and f'' at some $\eta \ll 1$. We started off at $\eta = \eta_0 = 0.001$, where we set

$$f = a_1\eta + a_2\eta^2 + a_3\eta^3 + a_4\eta^4 + a_5\eta^5. \tag{12}$$

If we substitute (12) in (11), expand about the origin of the η plane and, in the resulting expression, equate to zero successively the coefficients of ascending powers of η we find that for a prescribed c, specifying a_1, the coefficients of η^0, η, η^2 and η^3 yield, respectively, the terms a_2, a_3, a_4 and a_5. Thus for a prescribed c we can guess an $a_1 = f'(0)$ and compute a solution of (11) that satisfies the condition $f(0) = 0$. For the solution (i) $a_1 = c$ and for the solution (iii) $a_1 = -c - 2$. We used these solutions as a test of our computer programme, that is for a set of values of c we set $a_1 = c$ or $a_1 = -c - 2$. For $a_1 = c$, our programme produced the solution (i) and for $a_1 = -c - 2$ it produced the solution (iii).

We are interested in solutions that also satisfy the condition $f(\infty) = \text{constant}$, $f'(\infty) = 0$. Our computations indicated that these (additional) conditions are satisfied provided $c > 0$ and

$$-c - 2 < a_1 < c + 1. \tag{13}$$

The convergence of the solution is slow when $c = O(1)$ and it decreases as c decreases. It does appear that for $c < 0$ only the solution (i) satisfies the condition $f'(\infty) = 0$. For $c < 0$ the solution (i) relates to a down-draught and a radial outflow and is not realistic for tornado vortices. This type of solution will be ignored and in the discussion that follows we assume that $c > 0$.

If $a_1 = c + 1$, $f(\eta) = (c + 1)\eta$ (solution (ii)) and if $a_1 = -c - 2$, $f(\eta) \simeq (c + 1)\eta$ as $\eta \to \infty$, whereas if a_1 satisfies (13) $f(\infty) = \text{finite constant}$. This suggests that if a_1 satisfies (13) and is close to $c + 1$ or to $-c - 2$, then as $\eta \to \infty$ $f(\eta)$ tends to a finite large positive constant. This implies that if a_1 is close to $-c - 2$ (and satisfies (13)) $f(\eta) > 0$ for $\eta \gg 1$ and $f(\eta) < 0$ for $\eta \ll 1$. Details of our computations showed that, for $a_1 > 0, f(\eta) > 0$ (except at $\eta = 0$), that is we have a one-cell solution and for $a_1 < 0, f(\eta) < 0$ for small η and it changes sign once so that $f(\eta) > 0$ for large η and this corresponds to a two-cell vortex. The solutions (ii) and (iii) represent, respectively, the limiting forms of the one- and two-cell solutions. The function $f'(\eta)$ which relates to the axial velocity can be of constant sign or it can change sign one or more

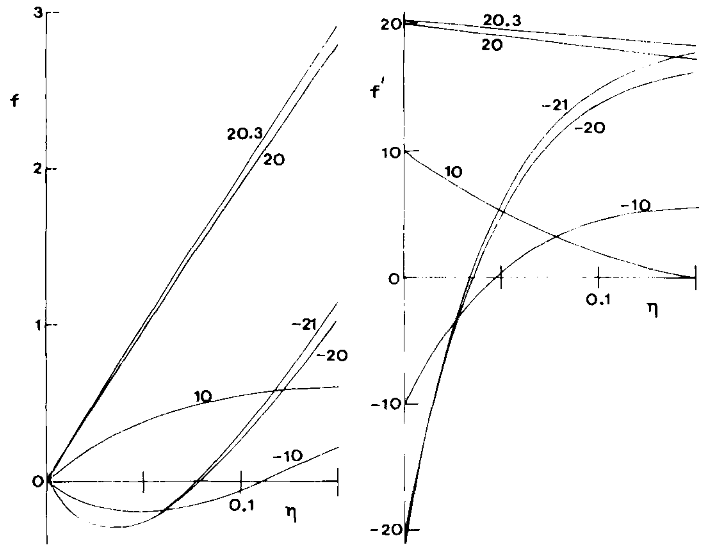

Fig. 1. Value of $f(\eta)$ and $f'(\eta)$ in the range $0 \leqslant \eta \leqslant 0.15$ for some $a_1 = f'(0)$ for the case $c = 20$. The numbers on the curves are values of a_1.

times and the latter case seems to occur when $a_1 < c$. When $f'(\eta)$ changes sign so does the vertical velocity w_0, that is there are solutions for $a_1 < c$ representing a series of up-draughts and down-draughts. The behaviour of $f(\eta)$ and $f'(\eta)$ is illustrated in Figs. 1 and 2 which show these functions for some a_1 for the case $c = 20$. Fig. 1 relates to the range $0 \leqslant \eta \leqslant 0.15$ and Fig. 2 relates to the range $0.1 \leqslant \eta \leqslant 4$. For large c, say $c = O(10)$, in the case of a two-cell solution $f(\eta)$ is negative only for a range of η satisfying the condition $\eta \ll 1$. This observation is illustrated in Fig. 1 for the curves referring to $a_1 = -10, -20$ and -21.

The solution of (7), subject to $M_0(0) = 0$, $M_0(\infty) = \Gamma_t/hV$, yields

$$Rv_0 = \frac{\Gamma_t}{hV} \int_0^\eta g(x)\mathrm{d}x \Big/ \int_0^\infty g(x)\mathrm{d}x, \tag{14}$$

where $g(x) = \exp\left[-x - \int_0^\eta (f(x)/x)\mathrm{d}x\right]$.

Note that for this similarity model the circulation Γ_t affects only the magnitude of v and has no influence on the structure of the flow field.

Following Bellamy-Knights and Saci we take, in SI units, $h = 4 \times 10^3$, $V = 40$, $\nu = 5$ and hence $\nu_1 = 10^{-4}/3.2$. These solutions are applicable to tall slender vortices and we assume that they extend to $r = 600$ m, then the range of interest is $0 < R = r/h < 0.15$ and $0 < Z = z/h \leqslant 1$. Kendall assumed that $c_1 \neq 0$ and used a scale length of 866.025 and a reference velocity $V = 8.66025$ for his solution given by (iii). Now $t'_0 = Vt_0/h$ and for $a_0 = 1$, $c_1 = 0$, $t'_0 = \Lambda$. Bellamy-Knights and Saci (1983), for $c_1 = 0$, chose $c \simeq t'_0 = 20$ and applied the solution (i), which corresponds to setting our $a_1 = 20$, to a diffusing atmospheric vortex such that the circulation at $r = \infty$, say Γ_t, is 7500. This means that $M_0(\infty) = \Gamma_t/hV$. They used this set of data to model the tangential velocity of the Dallas tornado (Hoecker, 1960), assuming that the diffusion process starts off at time t_0. For comparison we also set $c = t'_0 = 20$ and the results and discussion that follow relate to the case $c = 20$. For a numerical solution the only restriction on a_1 is that it satisfies (13) that is, for $c = 20$, $-22 < a_1 < 21$.

Figs. 3, 4 and 5 show respectively, the axial, radial and azimuthal velocities at $t' = 20$, 40 and 60 for $a_1 = 20.3$, 20 and -21. The case $a_1 = 20$ represents the analytical solution (i) and the case $a_1 = -21$ represents a two-cell solution. The dimensional time t is given by $t = ht'/V$ and thus

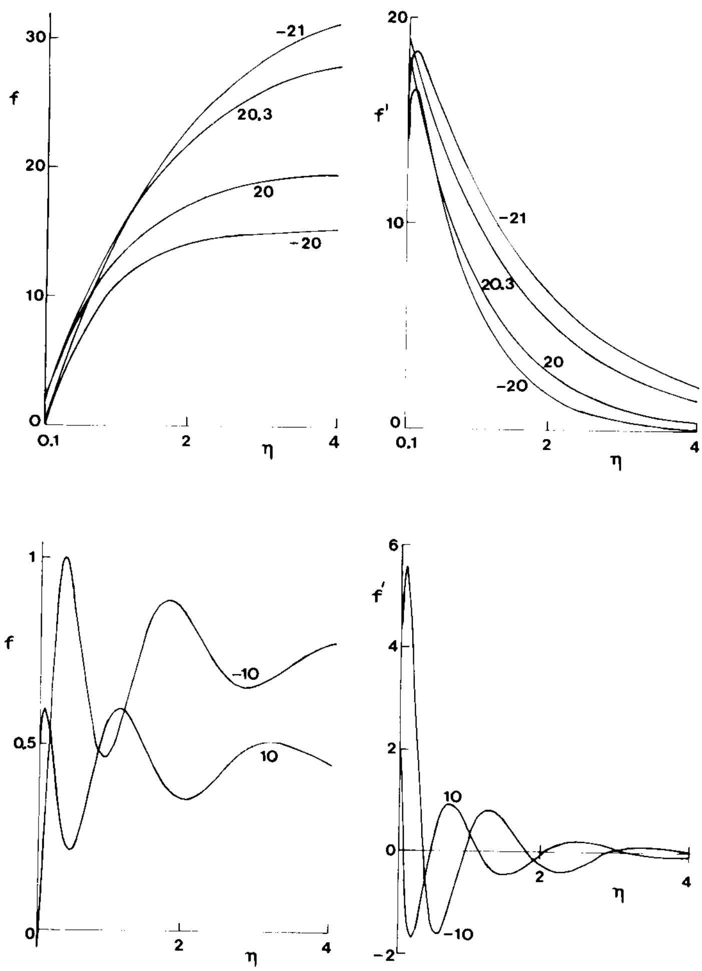

Fig. 2. Values of $f(\eta)$ and $f'(\eta)$ in the range $0.1 \leqslant \eta \leqslant 4$ for some a_1 for the case $c = 20$. The numbers on the curves are values of a_1. The values of $f(\infty)$ corresponding to $a_1 = 20.3$, 20, 10, -10, -20 and -21 are, respectively, 30.4, 20, 0.457, 0.746, 15.4 and 35.5.

the values $t' = 20$, 40 and 60 correspond to time $t = 2000$ s, 4000 s and 6000 s, respectively. It is evident from these figures (and also from Figs. 1 and 2) that, due to the nonlinearities of the problem, the choice of a_1 is of crucial importance for both the quantitative and qualitative description of the flows described by the similarity equations. It is seen from Fig. 3a, for example, that there is a substantial quantitative difference in the distribution of the vertical velocity between the cases $a_1 = 20$ and $a_1 = 20.3$. Also as a_1 tends to its maximum value of 21 the vertical velocity profiles become more flat. Fig. 3b refers to a two-cell solution and shows that near the axis there is a large down-draught which is followed by an up-draught. The up-draught reaches a maximum and thence it decreases (since $w_0 \to 0$ as $R \to \infty$). Fig. 3b is qualitatively similar to the corresponding figure constructed by Kendall (his Fig. 2), the main difference is that in Kendall's diagram $w_0 \to \text{constant} \neq 0$ as $R \to \infty$. As t' increases the overall magnitude of w_0 decreases and in the case of a two-cell solution the down-draught region expands.

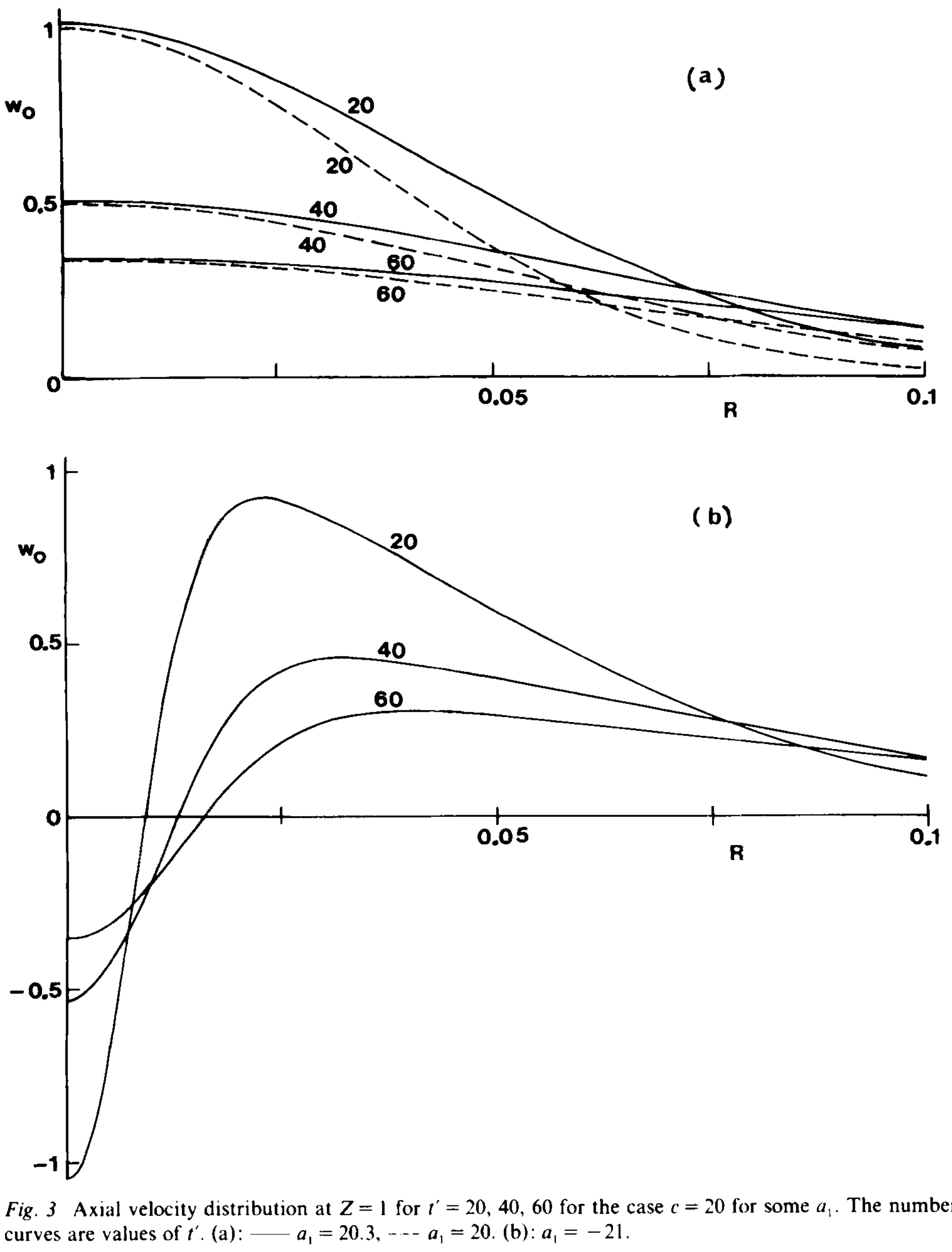

Fig. 3 Axial velocity distribution at $Z = 1$ for $t' = 20, 40, 60$ for the case $c = 20$ for some a_1. The numbers on the curves are values of t'. (a): —— $a_1 = 20.3$, - - - $a_1 = 20$. (b): $a_1 = -21$.

Fig. 4a shows the distribution of the radial velocity u_0 for one-cell vortices representing inflow. The magnitude of u_0 reaches a maximum and thence it decreases and tends to zero at large R. Again note the substantial difference in the overall magnitude of u_0 between the cases for $a_1 = 20$ and $a_1 = 20.3$. Fig. 4b shows u_0 for the case $a_1 = -21$ which represents a two-cell vortex. About the origin u_0 is positive and this represents outflow whereas away from it u_0 is negative which means that there is inflow. Note that the function u_0 has a maximum and a minimum and since $f(\infty) = \text{constant}$, $u_0 \to 0$ as $R \to \infty$.

Fig. 5 illustrates the tangential velocity v_0 and

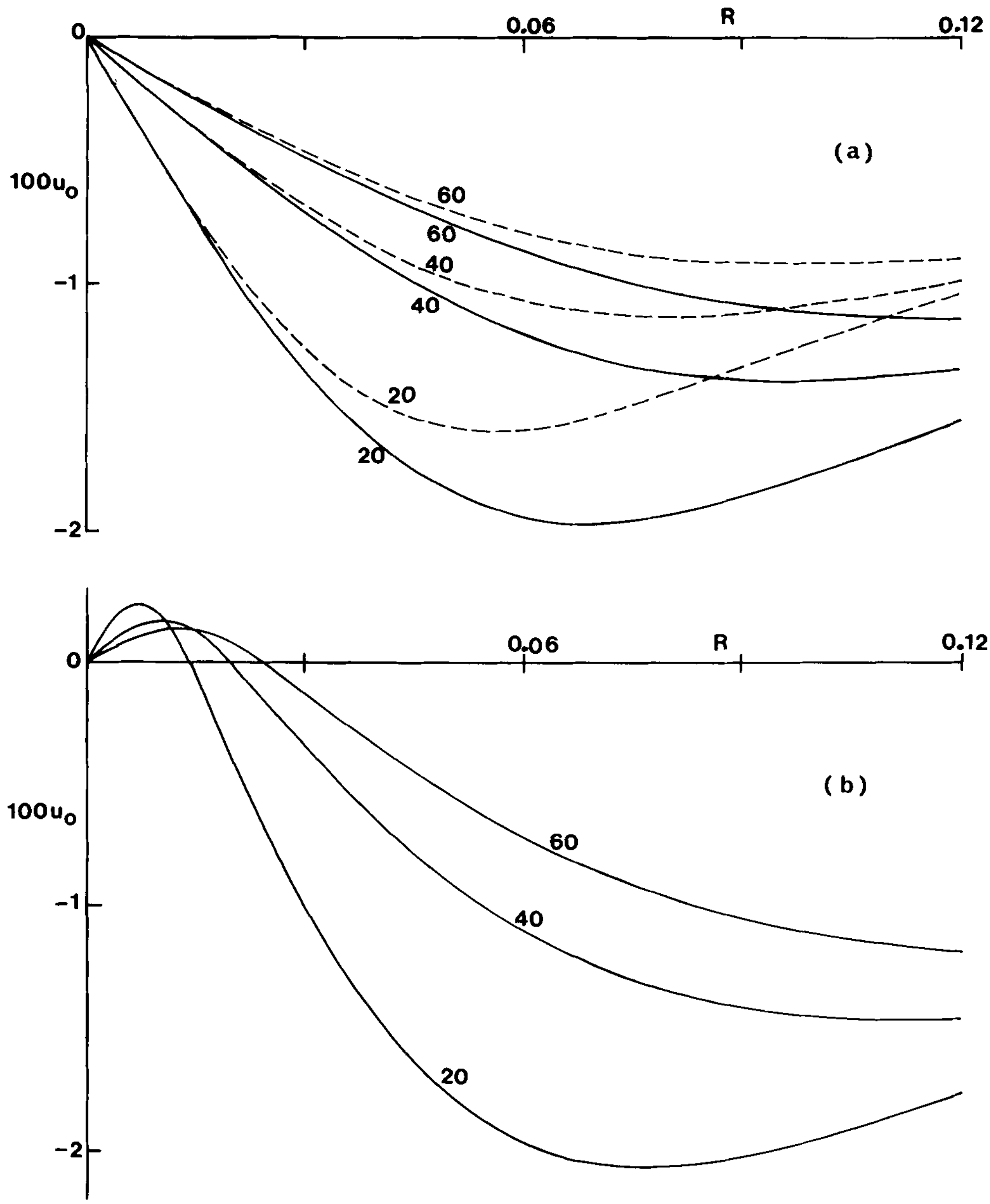

Fig. 4. Radial velocity distribution for $t' = 20, 40, 60$ for the case $c = 20$ for some a_1. The numbers on the curves are values of t'. (a): —— $a_1 = 20.3$, --- $a_1 = 20$. (b): $a_1 = -21$.

shows that this component of the velocity is qualitatively the same for both the one- and two-cell solutions, that is it reaches a maximum at some distance from the axis and thence it decreases and tends to zero at large R. As t' increases the maximum is depressed and it occurs further away from the axis. The overall profile of the tangential velocity resembles that of a Rankine vortex which is smoothed out at the edge of the core. Fig. 5a indicates that v_0, in contradistinction to u_0 and w_0, is not very sensitive to the choice of a_1. Detailed computations confirmed this observation for both the one- and two-cell vortices. For the one-cell vortex, we

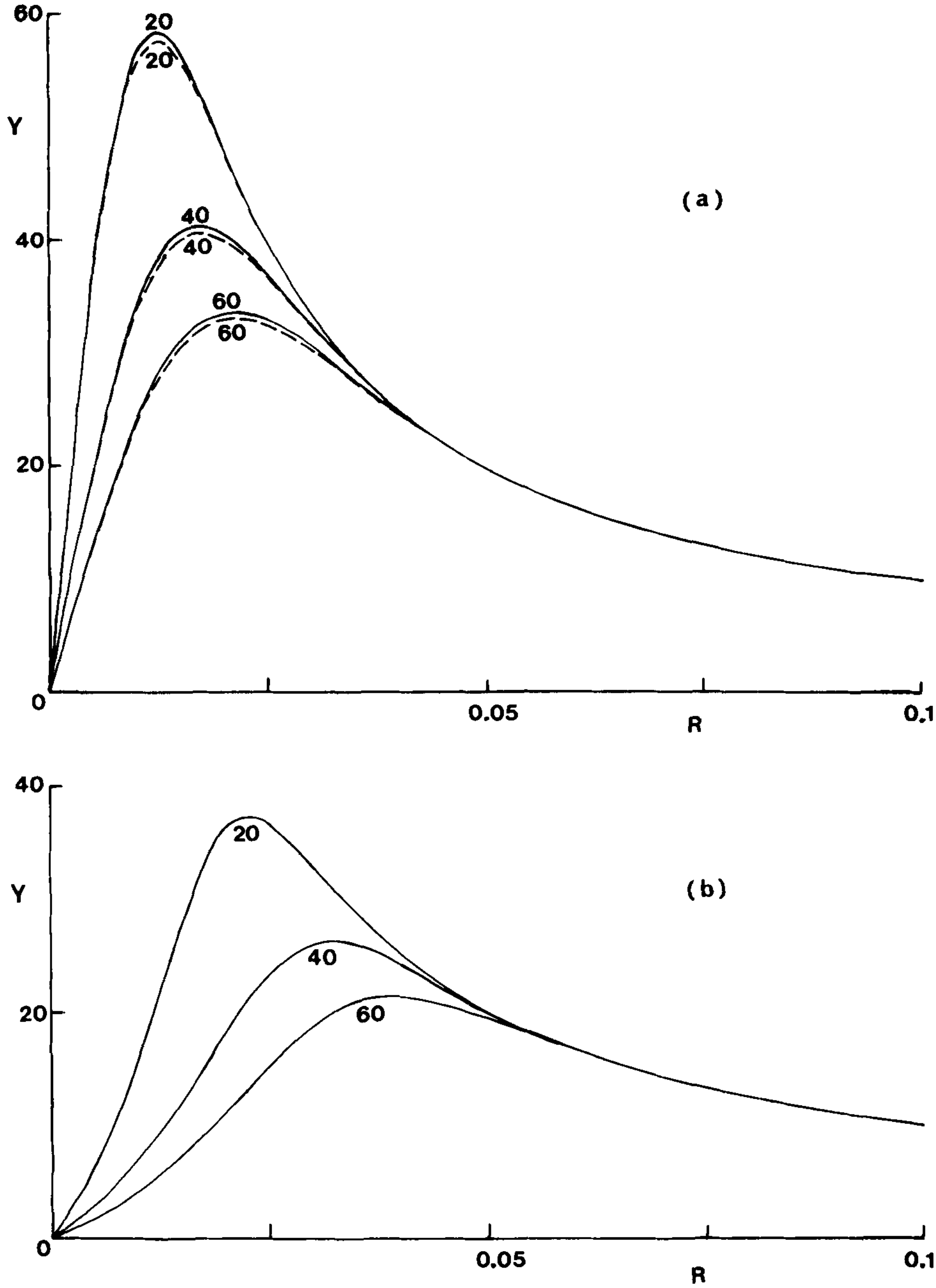

Fig. 5. Azimuthal velocity distribution for $t' = 20, 40, 60$ for the case $c = 20$ for some a_1. The numbers on the curves are values of t'. $Y = hVv_0/\Gamma$, $\simeq 21.3v_0$. (a): —— $a_1 = 20.3$, --- $a_1 = 20$. (b): $a_1 = -21$.

increased a_1 from 19 to its limiting value of 21 and found that at a particular time the function v_0 increased by less than 16% at every point and the radial position where the tangential velocity attains its maximum value v_m decreased by about 7%. At $t = 2000$ s, we find that for $a_1 = 19$, v_m

$\simeq 102$ ms^{-1} at $r \simeq 51.6$ m and for $a_1 = 21$, $v_m \simeq 112$ ms^{-1} at $r \simeq 48.3$ m, whereas at $t = 6000$ s for $a_1 = 19$, $v_m \simeq 59.0$ ms^{-1} at $r \simeq 89.3$ m and for $a_1 = 21$, $v_m \simeq 64.5$ ms^{-1} at $r = 83.6$ m. For the two-cell vortex we decreased a_1 from -20 to its limiting value of -22 and found that v_0 increased by less than 10% at every point and the radial position associated with v_m decreased by about 5%. At $t = 2000$ s for $a_1 = -20$, $v_m \simeq 67.9$ ms^{-1} at $r \simeq 92.6$ m and for $a_1 = -22$, $v_m \simeq 71.7$ ms^{-1} at $r \simeq 88.9$, whereas at $t = 6000$ s for $a_1 = -20$, $v_m \simeq 39.2$ ms^{-1} at $r \simeq 163$ m and for $a_1 = -22$, $v_m \simeq 41.4$ at $r \simeq 154$ m. Thus the changes in v_0 are of the order of the changes in the value of the parameter a_1, whereas small changes in a_1, say from 20 to 20.3, produce comparatively large changes in u_0 and w_0. This means that, due to the nonlinearities of the problem, small changes in the tangential velocity of the vortex can result in abnormally large changes in the associated radial and vertical velocities of the system.

The values of v_m mentioned here and of the tangential velocity v inferred from Fig. 5 ($v = 40v_0 \simeq 2Y$ ms^{-1}) are consistent with the tangential velocities measured in tornado vortices. Hoecker, for example, measured a maximum tangential velocity of 75 ms^{-1} at a distance of 40 m from the axis of the funnel for the 2 April 1957 Dallas tornado. Other tornado measurements can be found on pp. 210–212 of the article by Davies-Jones. These confirm that the values of v_m mentioned here are typical tangential velocities for tornadoes. Near the ground, however, the observational values of vertical and radial velocities are much larger than those relating to the vortices studied here which predict, for example, radial velocities of order 0.5 ms^{-1}. Also the time scale for the diffusion of the vortices studied here is larger than the life span of the tornadoes.

We finally attempted to construct solutions to (8) and (9) without the restriction $\sigma = cf'$ and also without the restriction $k_1 = v_1$. Our numerical experiments indicated that there may be solutions to (18) and (19) without the imposed restrictions, but the system, which is in effect a fifth order nonlinear differential equation, is highly unstable and it is difficult to construct these solutions.

4. Acknowledgements

The programming and computations of this paper were carried out by Mrs. L. C. Wilkinson.

REFERENCES

Bellamy-Knights, P. G. and Saci, R. 1983. Unsteady convective atmospheric vortices. *Boundary-Layer Meteorol. 27*, 371–386.

Davies-Jones, R. P. 1986. Tornado Dynamics. In *Thunderstorms morphology and dynamics*. (ed. E. Kessler). Oklahoma: University Press, 197–236.

Kendall, W. M. 1978. Unsteady two-cell similarity solution to a convective atmospheric vortex model. *Tellus 30*, 376–382.

Hoecker, W. H., Jr. 1960. Wind Speed and airflow patterns in the Dallas Tornado of April 2 1957. *Monthly Weather Rev. 88*, 167–180.

Kuo, H. L. 1966. On the dynamics of convective atmospheric vortices. *J. Atmos Sci. 23*, 25–42.